

# Advanced Tokamak Research in JT-60U and JT-60SA

Akihiko ISAYAMA for the JT-60 team

Japan Atomic Energy Agency, Naka, Ibaraki 311-0193, Japan

Results of experiment in JT-60U and design study in JT-60SA (Super Advanced) are described focusing on the development of advanced tokamak. In JT-60U, a high-integrated performance plasma with the normalized beta  $\beta_N=2.6$ , confinement enhancement factor  $H_{H98(y,2)}=1.0-1.1$  and bootstrap current fraction  $f_{BS}=0.4$  has been sustained for 25 s (14 times current diffusion time ( $\tau_R$ )). Neoclassical tearing mode (NTM) with the poloidal mode number  $m = 2$  and the toroidal mode number  $n = 1$  has been stabilized with modulated electron cyclotron current drive (ECCD) in synchronization with the mode frequency ( $\sim 5$  kHz). A high-beta plasma exceeding the ideal MHD limit without conducting wall has been sustained for 5 s ( $\sim 3\tau_R$ ) by suppressing resistive wall mode (RWM). In addition, two new instabilities in the high-beta regime, *Energetic particle driven Wall Mode* (EWM) and *RWM precursor*, have been observed. In JT-60SA, exploration of full non-inductive steady-state operation with current drive by neutral beams and electron cyclotron waves is planned. In addition, NTM control with ECCD and RWM suppression with external coils are planned.

Keywords: advanced tokamak, ITER, Hybrid Scenario, NTM, RWM, JT-60U, JT-60SA

## 1 Introduction

Steady-state sustainment of high integrated performance is essential for a fusion reactor, where simultaneous achievement of high values of the normalized beta ( $\beta_N$ ), confinement enhancement factor ( $H_{H98(y,2)}$ ), non-inductive current drive fraction ( $f_{NI}$ ) and so on is required. For example, in one of the advanced scenarios in ITER, so called the Hybrid Scenario,  $\beta_N=2-2.5$ ,  $H_{H98(y,2)}=1-1.2$  and  $f_{NI}=0.5$  are assumed to obtain the fusion gain  $Q\sim 5$  with the discharge duration of longer than 1000 s [1]

To develop the scenario of the advanced tokamak operation and clarify physics issues and their solution, advanced tokamak research has been extensively performed in JT-60U by fully utilizing its capability. In JT-60U, two major scenarios have been developed for the advanced tokamak research [2]: high- $\beta_p$  H-mode scenario and reversed shear scenario. Sustainment of high-performance plasmas for longer than current diffusion time have been achieved in both scenarios. This paper focuses only on the advanced tokamak research with high- $\beta_p$  H-mode.

In obtaining a stationary high-beta plasma, one of the magnetohydrodynamic (MHD) instabilities to be suppressed or controlled is a neoclassical tearing mode (NTM). The NTM is destabilized by bootstrap current in a plasma with positive magnetic shear and degrades the plasma performance. Among possible mode numbers, NTMs with  $m/n=3/2$  and  $2/1$  should be controlled since confinement degradation by them is large. Here,  $m$  and  $n$  are the poloidal and toroidal mode numbers, respectively.

In JT-60U, two scenarios for NTM suppression have been developed. One is avoidance of NTM onset through the optimization of pressure and current profiles. To be more specifically, the location of steep pressure gradient,

which is typically located at 0.3–0.7 in the averaged minor radius, is adjusted so that it is far from the mode rational surfaces. This scenario is advantageous in that NTMs can be suppressed without additional heating/current drive systems other than those for the high-performance plasma. In JT-60U, systems for plasma control, heating/current drive and diagnostics were upgraded to obtain a long-duration plasma with auxiliary heating using neutral beams (NBs) and electron cyclotron (EC) waves up to 30 s in 2003 [3,4]. After the installation of ferritic steel tiles in 2005, a higher-confinement plasma was obtained through the reduction of fast ions [5, 6]. In 2007, pulse width of 3 units of the perpendicular NBs was extended to 30 s, which enabled central plasma heating for longer time.

The other scenario for NTM suppression is active stabilization using electron cyclotron current drive (ECCD). In JT-60U, NTM stabilization has been performed since the installation of the first 110 GHz gyrotron in 1999 [7], and stabilization by real-time mirror steering [8], preemptive stabilization [9] and simulation with the TOPICS code [10–12] have been performed.

In a higher beta regime above the ideal beta limit without conducting wall ('no-wall limit'), a resistive wall mode (RWM) appears and terminates the discharge. RWM had been observed in reversed shear discharges before the installation of the ferritic steel tiles [13]. After the installation of the ferritic steel tiles, RWM study in a positive-shear plasma, which requires higher NB power to reach the no-wall limit, became possible. Detailed scan of toroidal velocity utilizing the capability of various NB injection pattern in JT-60U, the minimum required toroidal rotation velocity was found to be 0.3% of the Alfvén velocity [14].

The operation of JT-60U was concluded with great success in August 2008. A superconducting tokamak, JT-60SA (Super Advanced), is being constructed to take

author's e-mail: isayama.akihiko@jaea.go.jp

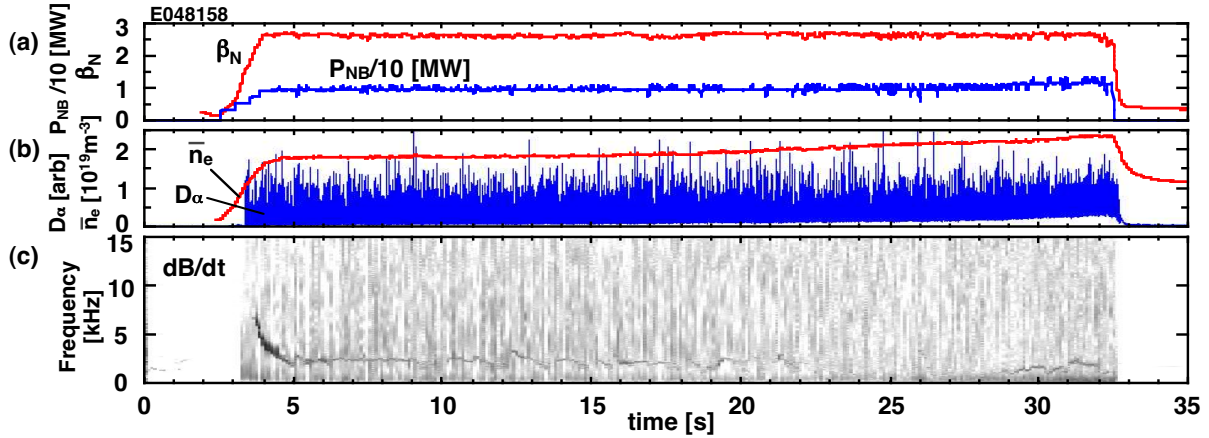


Fig. 1 Typical discharge of a long-pulse high-beta plasma. (a) Normalized beta and NB injection power, (b) line-averaged electron density and  $D_\alpha$  intensity, (c) frequency spectrum of magnetic perturbations.

over and drive forward the advanced tokamak research as a combined program of the ITER Satellite Tokamak Program of Japan and EU and the Japanese National Program.

This paper describes results from JT-60U experiments and JT-60SA design study with emphasis on advanced tokamak research. After this introduction, long-duration sustainment of a high-beta plasma through NTM avoidance is described in Sec. 2. Active stabilization of an  $m/n=2/1$  NTM with modulated ECCD is described in Sec. 3. Suppression of RWM by rotation control and newly observed instabilities are described in Sec. 3. Design and physics assessment in JT-60SA is described in Sec. 4. Finally, summary is described in Sec. 5.

## 2 Long-duration sustainment of high integrated performance plasma [15]

In JT-60U, the maximum pulse duration of 3 units of NBs was extended to 30 s in 2007, which enabled central heating for longer time. Typical discharge of a long-duration high-beta discharge is shown in Fig. 1. Plasma parameters in this discharge are as follows: the plasma current  $I_p=0.9$  MA, the toroidal field  $B_t=1.54$  T, the major radius  $R=3.36$  m, the minor radius  $a=0.88$  m, the plasma volume  $V_p=67$  m<sup>3</sup>, safety factor at 95% flux surface  $q_{95}=3.2$ . From  $t=2.5$  s neutral beam was injected stepwise to avoid onset of NTMs. The central value of safety factor  $q$  was nearly unity, but large sawtooth oscillation was not observed. The value of the normalized beta,  $\beta_N \equiv \beta_i / (I_p / a B_t)$ , reached 2.6 by about 10 MW NB injection, and was sustained by feedback control. It can be seen that the injection power is almost the same, and H-mode with edge localized mode (ELM) is sustained stationarily. From  $t \sim 20$  s,  $D_\alpha$  intensity and electron density gradually increased, and NB injection power slightly increased, showing confinement degradation. Frequency spectrum of magnetic perturbations (Fig. 1(c)) shows that no large instability such

as NTMs is observed throughout the discharge. Although infrequent sawtooth oscillations are observed at  $\sim 2$  kHz, confinement degradation is not visible. Profiles of ion and electron temperatures and safety factor at  $t=27$  s are shown in Fig. 2. While the temperature gradually decreased as the electron density increased, peaked profiles were maintained until the end of the high-beta phase. In addition, internal and edge transport barriers were also maintained. It can be seen that the  $q=1.5$  and 2 surfaces are located at the peripheral region with small temperature gradient, which is effective in avoiding NTM onset.

The value of confinement enhancement factor against the H-mode scaling,  $H_{H98(y,2)}$ , is 1.0–1.1, and the fraction of bootstrap current to the total plasma current,  $f_{BS}$ , is 0.43–0.46 from ACCOME code calculation. These parameters satisfy the requirement for the ITER Hybrid Scenario [1]. Current diffusion time,  $\tau_R$ , is 1.8 s. Here,  $\tau_R \equiv \mu_0 \langle \sigma \rangle a^2 / 12$ ,  $\mu_0$  is permeability and  $\langle \sigma \rangle$  is volume-averaged neoclassical conductivity [16]. Thus, the sustained period in Fig. 1 corresponds to about  $14\tau_R$ . Actually, safety factor profile measured with motional Stark effect diagnostic is fully relaxed and flat  $q$ -profile with  $q(0) \sim 1$  is sustained stationarily.

Progress in long-duration sustainment of high-beta plasma is shown in Fig. 3. Before 2003, confinement was not high ( $H_{H98(y,2)} \sim 0.8$ – $0.9$ ) although pulse duration was significantly increased from 10 to 30 s, and  $\beta_N=2.3$  was sustained for 22.3 s [3, 4]. Insertion of ferritic steel tiles contributed to extending the pulse duration as well as enhancing the confinement by reducing loss power and thus increasing available power in the later phase of discharges. Extension of the pulse width of the 3 perpendicular NBs in 2007 made it possible to further extend the duration of high-beta plasma, and as shown in Fig. 3,  $\beta_N=2.6$  was sustained for 25 s, and  $\beta_N=2.3$  was sustained for 28.6 s. Since the maximum pulse duration in the present JT-60U system is 30 s, the sustained period is nearly equal to the maximum pulse width of the NBs.

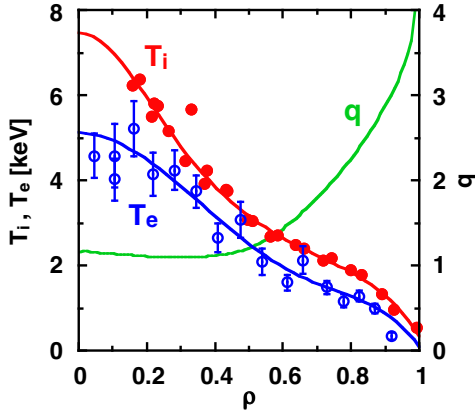


Fig. 2 Profiles of ion and electron temperatures and safety factor at  $t=27$  s.

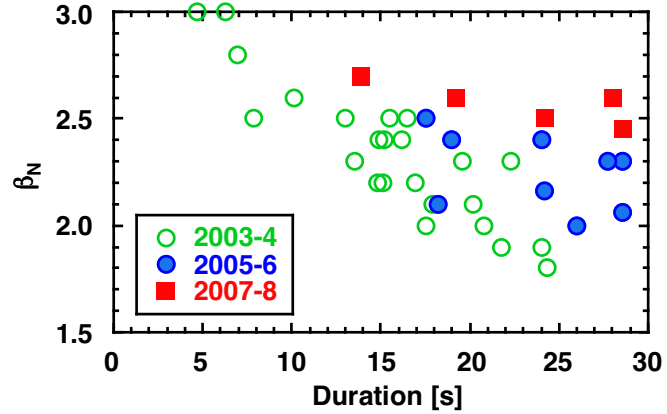


Fig. 3 Progress in the duration of a high beta plasma. Open circles, closed circles and closed squares correspond to the result in 2003–4, 2005–6 and 2007–8, respectively.

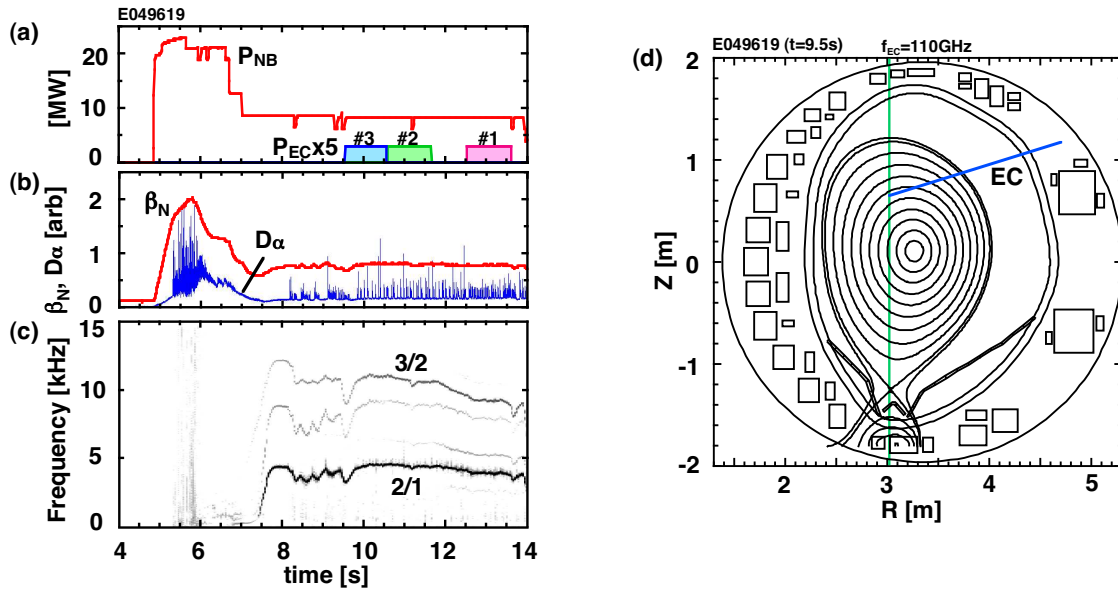


Fig. 4 Typical discharge of stabilization of an  $m/n=2/1$  NTM with ECCD. (a) Injection power of NB and EC wave, (b) the normalized beta and  $D_\alpha$  intensity, (c) frequency spectrum of magnetic perturbations, (d) plasma cross section. In Fig. 4(d), contour is drawn every 0.1 in the volume-averaged normalized minor radius.

### 3 Active stabilization of neoclassical tearing mode by localized electron cyclotron current drive [17]

In JT-60U, modulation frequency of gyrotrons has been increased year by year through continuous modification and conditioning. In 2008, modulation at about 7 kHz was successfully achieved [18, 19]. For NTM stabilization with modulated ECCD, EC wave is needed to be synchronized with the rotation of the NTM. In JT-60U, magnetic probe was used to generate a trigger signal for the modulation of gyrotron power. In addition, control system for the gyrotrons has been upgraded so that modulation frequency can be changed automatically by monitoring the magnetic probe signal in real time [19]. By using this sys-

tem, phase difference between the magnetic perturbations and the modulated EC wave power can be fixed even if the NTM frequency changes in time during a discharge [19]. In 2008, stabilization of an  $m/n=2/1$  NTM with modulated ECCD was performed.

Typical discharge waveform and plasma cross section in an NTM stabilization experiment are shown in Fig. 4, where typical plasma parameters are as follows:  $I_p=1.5$  MA,  $B_t=3.7$  T,  $R=3.18$  m,  $a=0.80$  m,  $q_{95}=4.1$ . In this series of discharges, NBs of about 25 MW was injected to destabilize a  $2/1$  NTM, and  $\beta_N$  increased to about 2. An  $m/n=2/1$  NTM appeared at  $t\sim 5.7$  s, and the value of  $\beta_N$  decreased to about 1.2. At  $t=6.7\text{--}7$  s, NB power was decreased and the direction of the tangential NBs was changed from balanced injection to counter injection to raise the mode frequency. The  $2/1$  NTM started to rotate

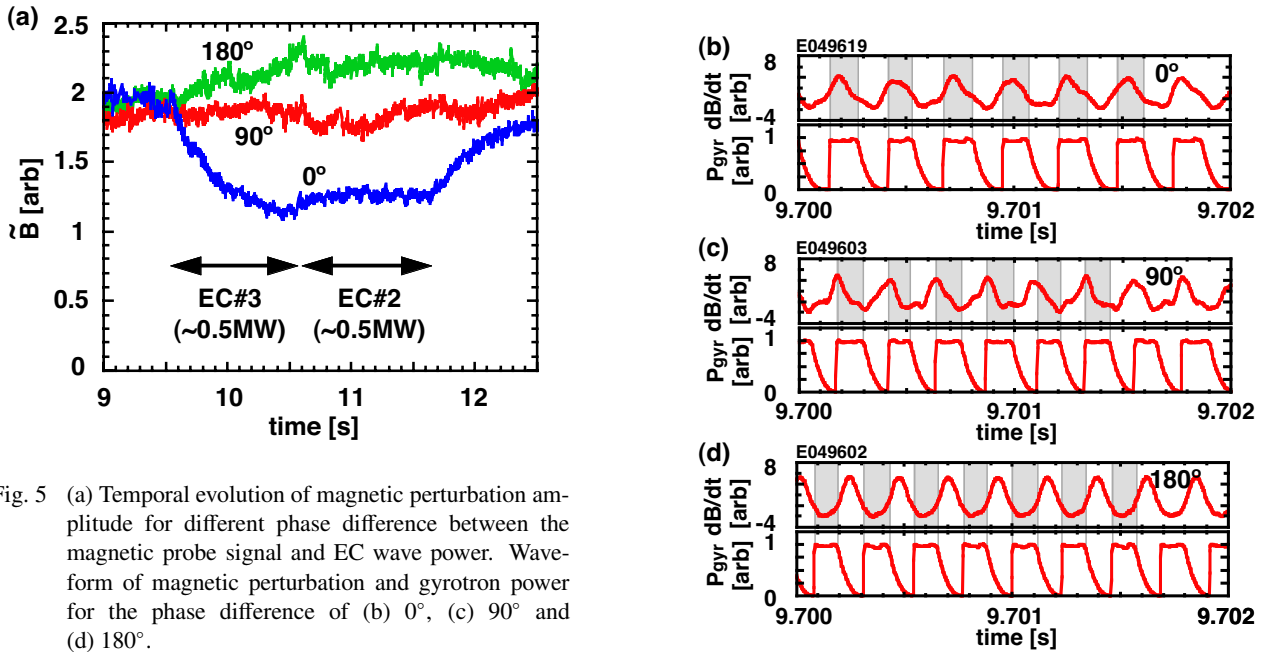


Fig. 5 (a) Temporal evolution of magnetic perturbation amplitude for different phase difference between the magnetic probe signal and EC wave power. Waveform of magnetic perturbation and gyrotron power for the phase difference of (b)  $0^\circ$ , (c)  $90^\circ$  and (d)  $180^\circ$ .

in the counter direction at  $t=7.5$  s, and the mode frequency reached about 4–5 kHz as shown in Fig. 4(c). Electron cyclotron wave with the frequency of 110 GHz was injected at  $t=9.5$  s from the low-field side as shown in Fig. 4(d). The 2/1 mode is located at  $\rho \sim 0.6$ , where  $\rho$  is volume averaged normalized minor radius. According to calculation with ACCOME and EC-Hamamatsu codes, the total EC-driven current is 3 kA, and the peak EC-driven current density corresponds to  $\sim 20\%$  of bootstrap current density at the  $q=2$  surface.

Temporal evolution of magnetic perturbation amplitude is shown in Fig. 5(a), where phase difference between magnetic probe signal and gyrotron power  $P_{\text{gyr}}$  is  $0^\circ$ ,  $90^\circ$  and  $180^\circ$ . For the  $0^\circ$  case, the mode amplitude decreases during the ECCD. For the  $90^\circ$  case, no clear effect of ECCD is seen, and for the  $180^\circ$  case, increase of mode amplitude, that is, NTM destabilization is observed. Detailed scan of the phase difference shows that O-point ECCD corresponds to the case when the phase difference is about  $-10^\circ$ . Thus, the  $0^\circ$  case and the  $180^\circ$  nearly correspond to O-point ECCD and X-point ECCD, respectively. From this figure, it can be seen that phase difference should be properly controlled to stabilize an NTM efficiently. Expanded figure of magnetic probe signal and gyrotron power for each case is shown in Figs. 5(b)–(d). As shown in these figures, the phase difference is successfully scanned by using the newly developed system. It was also found that the stabilization effect defined by the initial decay time of the magnetic perturbation amplitude increases with deviating from the optimum phase difference: the decay time is doubled when the deviation becomes  $\pm 50^\circ$ .

It is considered that modulated ECCD is more effective in stabilizing an NTM than unmodulated ECCD. However, experimental verification for an  $m/n=2/1$  NTM has

not been done yet. In JT-60U, it was found that the initial decay time for modulated ECCD is less than half of that for unmodulated ECCD with almost the same (peak) EC wave power. This shows that required EC wave power can be reduced significantly by modulating the EC wave.

#### 4 Long duration sustainment of high-beta plasmas above no-wall limit through resistive wall mode suppression [20]

In the 2008 campaign, experiments on high-beta plasmas above the no-wall limit are focused on the extension of the duration. Typical discharge of a high-beta discharge is shown in Fig. 6, where plasma parameters are as follows:  $I_p=0.9$  MA,  $B_t=1.44$  T,  $R=3.43$  m,  $a=0.91$  m,  $q_{95}=3.2$ . As shown in Fig. 6(a), the plasma volume is relatively large to enhance the wall stabilization effect, but not so large as to increase metal impurity from the wall. In this discharge, beta value was first increased by positive-ion-based NBs alone, and then some of the perpendicular NBs were turned off to replace with negative-ion-based NBs. The change of the injection pattern is effective in avoiding the instabilities which trigger RWMs (described later) by increasing in the plasma rotation velocity and at the same time reducing trapped particle component of fast ions. The value of the normalized beta was kept at  $\sim 3.0$  by feedback control on NBs. The no-wall beta limit,  $\beta_N^{\text{no-wall}}$ , calculated by an ideal MHD stability code MARG2D [21] is  $\sim 2.6$ , which corresponds to  $3.0\ell_i$ . Here,  $\ell_i$  is the internal inductance. The beta limit with an ideal wall,  $\beta_N^{\text{ideal-wall}}$ , is calculated to be  $\sim 3.2$  corresponding to  $3.8\ell_i$ . The value of

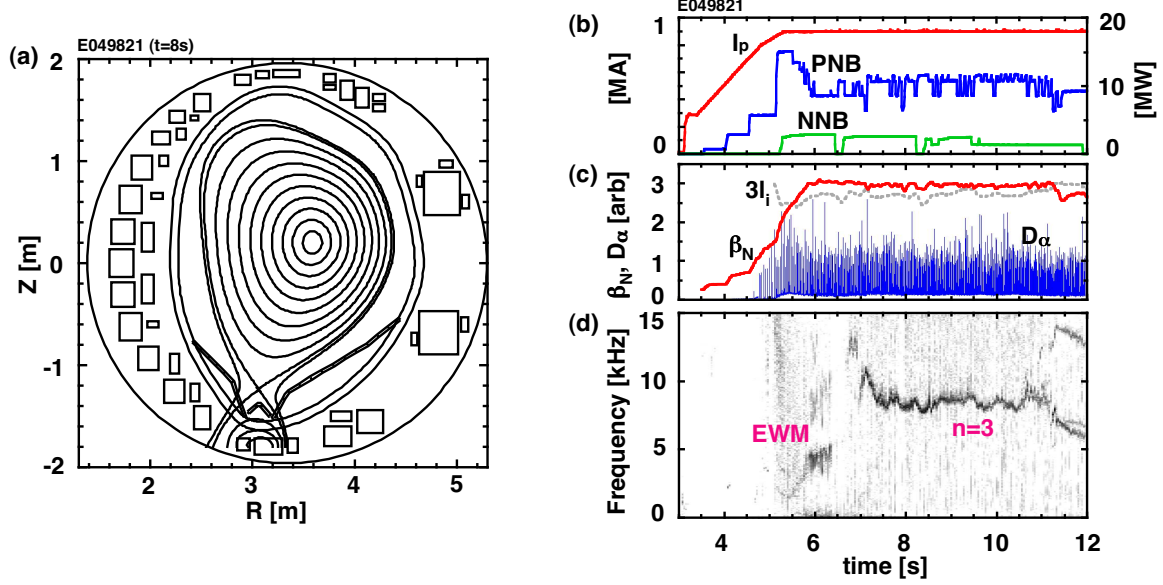


Fig. 6 Typical discharge of sustainment of a high-beta plasma above the no-wall limit. (a) Plasma cross section, (b) plasma current and injection power of NB, (c) normalized beta and  $D_\alpha$  intensity, (d) frequency spectrum of magnetic perturbations, .

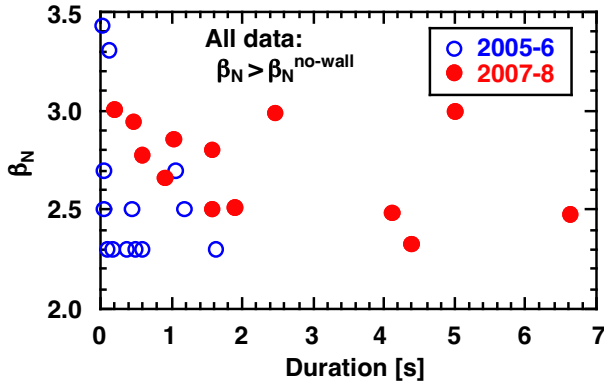


Fig. 7 Sustained value of the normalized beta versus duration. All data reach a beta value above the no-wall limit. Open circles and closed circles correspond to the data in 2005–6 and 2007–8, respectively.

$C_\beta \equiv (\beta_N - \beta_N^{\text{no-wall}}) / (\beta_N^{\text{ideal-wall}} - \beta_N^{\text{no-wall}})$ , which indicates how close to the ideal wall limit the beta value is, reaches about 0.3. In this discharge, the no-wall beta limit gradually increases in time due to current penetration and  $\beta_N$  becomes smaller than  $3\ell_i$  at  $t=11.2$  s. The duration of high beta above the no-wall limit is about 5 s, which corresponds to 3 times the current diffusion time. Progress in sustained duration of high-beta plasmas above the no-wall limit is shown in Fig. 7. Note that all of the data points are the ones with  $\beta_N > \beta_N^{\text{no-wall}}$ . Although the duration was limited to less than 1.6 s in 2005–6, it has been significantly extended in 2007–8.

In this series of discharges, two kinds of instabilities appeared and limited the discharge duration through the onset of RWM: one is a fishbone-like instability termed *Energetic particle driven Wall Mode* (EWM), and the other

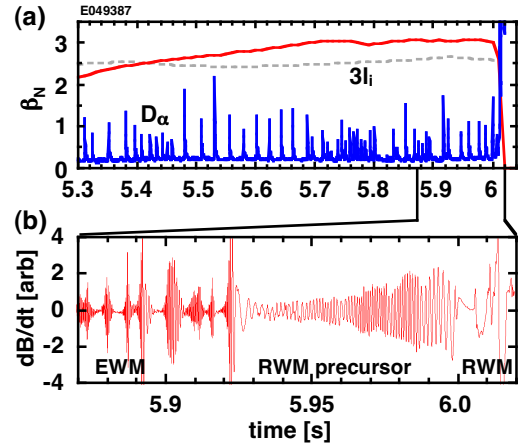


Fig. 8 Example of EWM and RWM precursor. (a)  $\beta_N$  and  $D_\alpha$  intensity and (b) expanded figure of magnetic perturbations.

is a slowly glowing mode termed *RWM precursor*. Both instabilities are observed only at  $\beta_N > \beta_N^{\text{no-wall}}$ , and one of them or both of them appeared in many of the high-beta discharges. Figure 8 shows an example where both EWM and RWM precursor are observed before an RWM. It is found that the EWM is triggered by an ELM or an EWM and has the following characteristics: (a) the growth and decay time are a few milliseconds, which is comparable to the resistive wall time  $\tau_w$ , (b)  $n=1$  and  $m=3-4$ , (c) no phase inversion in electron temperature measured with electron cyclotron emission diagnostics, that is, no island structure, (d) much larger amplitude at the low-field side than at the high-field side, (e) frequency chirping, (f) mode amplitude correlating with the power of perpendicular NBs. The EWM is different from the so-called fishbone instability in that the EWM is observed even when the central safety factor is above unity. The RWM precursor has the following

characteristics: (a) the growth time is 10–50 ms ( $\gg \tau_w$ ), (b)  $n=1$  and  $m=2-3$ , (c) no island structure, (d) a kink-ballooning-like mode structure, (e) it decreases  $V_t$  and/or  $dV_t/dr$ . In this series of experiments, it was found that the EWM appears and triggers RWM even when rotation velocity and its shear are enough high for RWM stability. In addition, the RWM precursor decreases the rotation velocity and its shear and triggers RWM. Thus, control of energetic particles and rotation velocity/shear was found to be important for RWM stability.

## 5 Physics assessment for JT-60SA

The JT-60SA device, equipped with toroidal and poloidal coils with superconducting magnets, will be installed in the present JT-60 torus hall [22, 23]. A birds-eye view of JT-60SA is shown in Fig. 9. The mission of JT-60SA is early realization of fusion energy by supporting exploitation of ITER and performing research toward DEMO. The maximum plasma current is 5.5 MA with a low aspect ratio ( $\sim 2.5$ ) plasma, and  $\sim 3$  MA for an ITER-shaped plasma. Inductive operation with a flat top duration up to 100 s will be possible within the total available flux swing. As in the JT-60U experiments, control of NTM and RWM is an important issue in JT-60SA. For RWM control, in-vessel coils are to be installed in addition to passive conducting wall. For NTM control, the 110 GHz EC wave system will be reused with improvements in the pulse width and power. Other components for the JT-60U facility, such as NB and diagnostic system, will be reused. Since the heating/current drive system is needed to be upgraded for the JT-60SA operation, R&D activities are being done in parallel with the construction.

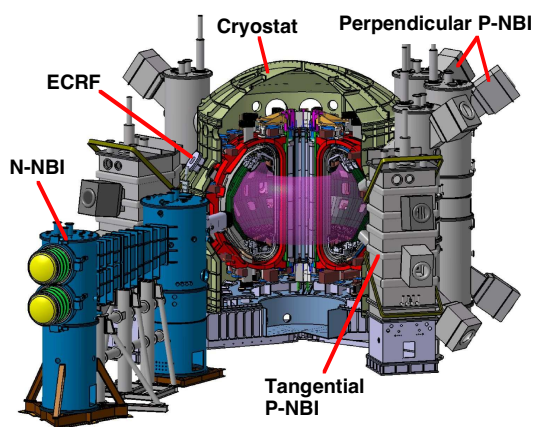


Fig. 9 Birds-eye view of JT-60SA.

## 6 Summary

Significant progress has been made in JT-60U advanced tokamak research until the very end of its experimental campaign in August 2008. A high-integrated performance

plasma with  $\beta_N \sim 2.6$ ,  $H_{H98(y,2)} = 1.0-1.1$ ,  $f_{BS} \sim 0.4$ , which satisfies the requirement of the ITER Hybrid Scenario, has been stationary sustained for 25 s ( $14\tau_R$ ). Stabilization of an  $m/n=2/1$  NTM with modulated ECCD has been successfully performed by modulating EC wave at  $\sim 5$  kHz in synchronization with mode frequency. The superiority of modulated ECCD to unmodulated ECCD by a factor more than 2 has been shown experimentally. A high-beta plasma above the no-wall limit has been sustained for  $\sim 5$  s ( $\sim 3\tau_R$ ). Two new instabilities which appear only at  $\beta_N > \beta_N^{\text{no-wall}}$ , energetic particle driven wall mode (EWM) and RWM precursor, have been observed. Design activity for JT-60SA is undergoing. Physics assessment is also being done for advanced tokamak research.

- [1] M. Shimada, D.J. Campbell, V. Mukhovatov *et al.*, Nucl. Fusion **47**, S1 (2007).
- [2] Y. Kamada, T. Fujita, S. Ishida *et al.*, Fusion Sci. Tech. **42**, 185 (2002).
- [3] S. Ide, the JT-60 team, Nucl. Fusion **45**, S48 (2005).
- [4] A. Isayama, the JT-60 Team, Phys. Plasmas **12**, 056117 (2005).
- [5] H. Takenaga, the JT-60 team, Nucl. Fusion **47**, S563 (2007).
- [6] N. Oyama, A. Isayama, T. Suzuki *et al.*, Nucl. Fusion **47**, 689 (2007).
- [7] Y. Ikeda, A. Kasugai, S. Moriyama *et al.*, Fusion Sci. Technol. **42**, 435 (2002).
- [8] A. Isayama, Y. Kamada, N. Hayashi *et al.*, Nucl. Fusion **43**, 1272 (2003).
- [9] K. Nagasaki, A. Isayama, S. Ide *et al.*, Nucl. Fusion **43**, L7 (2003).
- [10] N. Hayashi, A. Isayama, K. Nagasaki *et al.*, J. Plasma Fusion Res. **80**, 605 (2004).
- [11] K. Nagasaki, A. Isayama, N. Hayashi *et al.*, Nucl. Fusion **45**, 1608 (2005).
- [12] A. Isayama, N. Oyama, H. Urano *et al.*, Nucl. Fusion **47**, 773 (2007).
- [13] S. Takeji, S. Tokuda, T. Fujita *et al.*, Nucl. Fusion **42**, 5 (2002).
- [14] M. Takechi, G. Matsunaga, N. Aiba *et al.*, Phys. Rev. Lett. **98**, 055002 (2007).
- [15] N. Oyama, the JT-60 Team, Fusion Energy 2008 (Proc. 22nd IAEA Fusion Energy Conf., Geneva (IAEA, Vienna)) IAEA-CN-165/OV/1-3 (2008).
- [16] D.R. Mikkelsen, Phys. Fluids B **1**, 333 (1989).
- [17] A. Isayama, G. Matsunaga, T. Kobayashi *et al.*, Fusion Energy 2008 (Proc. 22nd IAEA Fusion Energy Conf., Geneva (IAEA, Vienna)) IAEA-CN-165/EX/5-4 (2008).
- [18] S. Moriyama, T. Kobayashi, A. Isayama *et al.*, Fusion Energy 2008 (Proc. 22nd IAEA Fusion Energy Conf., Geneva (IAEA, Vienna)) IAEA-CN-165/FT/P2-26 (2008).
- [19] T. Kobayashi, M. Terakado, F. Sato *et al.*, submitted to Plasma Fusion Res. (2008).
- [20] G. Matsunaga, Y. Sakamoto, N. Aiba *et al.*, Fusion Energy 2008 (Proc. 22nd IAEA Fusion Energy Conf., Geneva (IAEA, Vienna)) IAEA-CN-165/EX/5-2 (2008).
- [21] S. Tokuda, T. Watanabe, Nucl. Fusion **6**, 3012 (1999).
- [22] M. Kikuchi, Fusion Energy 2006 (Proc. 21st IAEA Fusion Energy Conf., Chengdu (IAEA, Vienna)) IAEA-CN-149/FT/2-5 (2006).
- [23] M. Matsukawa, M. Kikuchi, T. Fujii *et al.*, Fusion Eng. Design **83**, 795 (2008).